

UCSF

UC San Francisco Previously Published Works

Title

Whole-exome sequencing and imaging genetics identify functional variants for rate of change in hippocampal volume in mild cognitive impairment

Permalink

<https://escholarship.org/uc/item/6zh8g040>

Journal

Molecular Psychiatry, 18(7)

ISSN

1359-4184

Authors

Nho, K
Corneveaux, JJ
Kim, S
[et al.](#)

Publication Date

2013-07-01

DOI

10.1038/mp.2013.24

Peer reviewed

Published in final edited form as:

Mol Psychiatry. 2013 July ; 18(7): 781–787. doi:10.1038/mp.2013.24.

Whole-exome sequencing and imaging genetics identify functional variants for rate of change in hippocampal volume in mild cognitive impairment

K Nho¹, JJ Corneveaux², S Kim^{1,3}, H Lin³, SL Risacher¹, L Shen^{1,3}, S Swaminathan^{1,4}, VK Ramanan^{1,4}, Y Liu^{3,4}, T Foroud^{1,3,4}, MH Inlow⁵, AL Siniard², RA Reiman², PS Aisen⁶, RC Petersen⁷, RC Green⁸, CR Jack⁷, MW Weiner^{9,10}, CT Baldwin¹¹, K Lunetta¹², LA Farrer^{11,13}, SJ Furney^{14,15,16}, S Lovestone^{14,15,16}, A Simmons^{14,15,16}, P Mecocci¹⁷, B Vellas¹⁸, M Tsolaki¹⁹, I Kloszewska²⁰, H Soininen²¹, BC McDonald^{1,22}, MR Farlow²², B Ghetti²³, MJ Huentelman², and AJ Saykin^{1,3,4,22} for the Multi-Institutional Research on Alzheimer Genetic Epidemiology (MIRAGE) Study; for the AddNeuroMed Consortium; for the Indiana Memory and Aging Study; for the Alzheimer's Disease Neuroimaging Initiative (ADNI)²⁴

¹Department of Radiology and Imaging Sciences, Center for Neuroimaging, Indiana University School of Medicine, Indianapolis, IN, USA ²Neurogenomics Division, The Translational Genomics Research Institute (TGen), Phoenix, AZ, USA ³Center for Computational Biology and Bioinformatics, Indiana University School of Medicine, Indianapolis, IN, USA ⁴Department of Medical and Molecular Genetics, Indiana University School of Medicine, Indianapolis, IN, USA ⁵Department of Mathematics, Rose-Hulman Institute of Technology, Terre Haute, IN, USA ⁶Department of Neuroscience, University of California, San Diego, San Diego, CA, USA ⁷Mayo Clinic, Rochester, MN, USA ⁸Division of Genetics, Department of Medicine, Brigham and Women's Hospital and Harvard Medical School, Boston, MA, USA ⁹Department of Radiology, Medicine and Psychiatry, University of California, San Francisco, San Francisco, CA, USA ¹⁰Department of Veterans Affairs Medical Center, San Francisco, CA, USA ¹¹Biomedical Genetics, Boston University School of Medicine, Boston, MA, USA ¹²Department of Biostatistics, School of Public Health, Boston University, Boston, MA, USA ¹³Genetic Epidemiology Center, Boston University School of Medicine, Boston, MA, USA ¹⁴King's College London, Institute of Psychiatry, London, UK ¹⁵King's College London, NIHR Biomedical Research Centre for Mental Health at South London and Maudsley NHS Foundation Trust, Institute of Psychiatry, London, UK ¹⁶King's College London, NIHR Biomedical Research Unit for Dementia at South London and Maudsley NHS Foundation Trust, Institute of Psychiatry, London, UK ¹⁷Institute of Gerontology and Geriatrics, University of Perugia, Perugia, Italy ¹⁸Department of Geriatric Medicine, Gerontopole de Toulouse, Toulouse University Hospital, Toulouse, France ¹⁹Third Department of Neurology, Aristotle University of Thessaloniki, Thessaloniki, Greece ²⁰Department of Old Age Psychiatry and Psychotic Disorders, Medical University of Lodz, Lodz, Poland ²¹Department of Neurology, Kuopio University Hospital, University of Eastern Finland, Kuopio, Finland

© 2013 Macmillan Publishers Limited All rights reserved

Correspondence: Dr AJ Saykin, Department of Radiology and Imaging Sciences, Center for Neuroimaging, Indiana University School of Medicine, IU Health Neuroscience Center, Suite 4100, 355 West 16th Street, Indianapolis, IN 46202-3082, USA. asaykin@iu.edu.

²⁴Data used in preparation of this article were obtained from the Alzheimer's Disease Neuroimaging Initiative (ADNI) database (adni.loni.ucla.edu). As such, the investigators within the ADNI contributed to the design and implementation of ADNI and/or provided data but did not participate in analysis or writing of this report. A complete listing of ADNI investigators can be found at: http://adni.loni.ucla.edu/wp-content/uploads/how_to_apply/ADNI_Acknowledgement_List.pdf.

CONFLICT OF INTEREST

The authors declare no conflict of interest.

Supplementary Information accompanies the paper on the Molecular Psychiatry website (<http://www.nature.com/mp>)

²²Department of Neurology, Indiana University School of Medicine, Indianapolis, IN, USA and
²³Department of Pathology and Laboratory Medicine, Indiana University School of Medicine, Indianapolis, IN, USA

Abstract

Whole-exome sequencing of individuals with mild cognitive impairment, combined with genotype imputation, was used to identify coding variants other than the apolipoprotein E (*APOE*) 4 allele associated with rate of hippocampal volume loss using an extreme trait design. Matched unrelated *APOE* 3 homozygous male Caucasian participants from the Alzheimer's Disease Neuroimaging Initiative (ADNI) were selected at the extremes of the 2-year longitudinal change distribution of hippocampal volume (eight subjects with rapid rates of atrophy and eight with slow/stable rates of atrophy). We identified 57 non-synonymous single nucleotide variants (SNVs) which were found exclusively in at least 4 of 8 subjects in the rapid atrophy group, but not in any of the 8 subjects in the slow atrophy group. Among these SNVs, the variants that accounted for the greatest group difference and were predicted *in silico* as 'probably damaging' missense variants were rs9610775 (*CARD10*) and rs1136410 (*PARP1*). To further investigate and extend the exome findings in a larger sample, we conducted quantitative trait analysis including whole-brain search in the remaining ADNI *APOE* 3/3 group ($N=315$). Genetic variation within *PARP1* and *CARD10* was associated with rate of hippocampal neurodegeneration in *APOE* 3/3. Meta-analysis across five independent cross sectional cohorts indicated that rs1136410 is also significantly associated with hippocampal volume in *APOE* 3/3 individuals ($N=923$). Larger sequencing studies and longitudinal follow-up are needed for confirmation. The combination of next-generation sequencing and quantitative imaging phenotypes holds significant promise for discovery of variants involved in neurodegeneration.

Keywords

ADNI; *CARD10*; imaging genetics; mild cognitive impairment; *PARP1*; whole-exome sequencing

INTRODUCTION

Late-onset Alzheimer's disease (LOAD) is the most common age-related neurodegenerative disease and its incidence is rapidly increasing.¹ LOAD is marked by the presence of abnormal proteins forming histologically visible structures, plaques and tangles, which damage and destroy neurons.^{2,3} While the pathophysiology of LOAD is not fully understood, genetic factors have an important role in the development of LOAD. The heritability for LOAD is predicted to be as high as 80% based on twin studies.⁴⁻⁶ A number of association studies have evaluated genetic variants in LOAD.⁷⁻¹⁶ The 4 allele of apolipoprotein E (*APOE*) is the best established and the most significant genetic risk factor.¹⁷⁻¹⁹ Recent large-scale genome-wide association studies have identified and confirmed almost 10 additional genetic variants in multiple data sets,¹¹⁻¹⁶ which demonstrated population attributable fractions between 2.72 and 5.97%.¹⁵ The total proportion of heritability explained by the susceptibility genes including *APOE* is estimated to be 23%.²⁰

Nonetheless, a substantial proportion of the heritability for LOAD likely remains unexplained by the susceptibility genes identified so far. In addition, the majority of genetic variants identified by genome-wide association studies for LOAD were within non-coding regions. Rapid advances in high-throughput sequence capture methods and massively parallel sequencing technologies facilitate the search for disease-causing coding variants,

which are unlikely to be detected by genome-wide association studies.^{21–23} Recent studies using next-generation sequencing have successfully identified mutated genes underlying rare Mendelian disorders.^{24–26}

Since the cost of sequencing whole exomes in large cohorts is still high, alternative research strategies have been employed to reduce costs and to increase statistical efficiency.²² One approach is to select families that have multiple individuals affected with a common disease of interest (family-based design),^{24,27} and another is to select a small group of individuals that are at the extreme ends of a phenotypic trait distribution (extreme-trait design) due to rare, deleterious variants.²⁸

Whole-exome sequencing (WES) studies of AD published to date have focused on early-onset AD^{29,30} and have identified the causative genes in a small number of early-onset AD individuals. In contrast, analyses of WES or whole-genome sequencing (WGS) have not yet been reported in LOAD individuals. To date, resequencing studies of LOAD individuals have used target regions chosen by genomic selection strategies informed by genome-wide association studies.^{31,32} Sequencing selected protein-coding regions in large samples has led to the identification of multiple rare variants contributing to LOAD.^{31,32}

Amnesic mild cognitive impairment (MCI) is considered to be a precursor to the development of AD.³³ Subjects with amnesic MCI have a highly elevated probability of developing AD with approximately half converting to probable AD within 5 years.³⁴

Rate of neurodegeneration in MCI and ability to predict disease trajectory are extremely important. To study the genetic architecture of rate of change in imaging parameters, we performed WES of unrelated subjects with MCI using an extreme-trait design. Rate of longitudinal change of hippocampal volume over a 2-year period was selected as the quantitative trait to identify variants associated with medial temporal neurodegeneration, a hallmark of MCI and AD. In addition, we focused on subjects with MCI whose *APOE* genotype was $\epsilon 3/\epsilon 3$ to improve our power to detect novel variants rather than the well-described *APOE* $\epsilon 4$ effect. Finally, to investigate our exome findings further in a larger sample, we analyzed *APOE* $\epsilon 3/\epsilon 3$ participants by imputing identified variants in five independent cohorts. To our knowledge, this is the first study to use an extreme-trait approach toward identification of LOAD risk genes or neuroimaging measures as a quantitative trait for WES.

MATERIALS AND METHODS

Samples

All individuals used in this report were participants of the Alzheimer's Disease Neuroimaging Initiative Phase 1 (ADNI-1) and its subsequent extension (subsequent extension of ADNI), AddNeuroMed, Indiana Memory and Aging Study, and Multi Institutional Research on Alzheimer Genetic Epidemiology studies (Supplementary information). A majority of ADNI-1 participants (818 out of 822) were genotyped in 2009 using the Illumina Human610-Quad BeadChip. Genotyping and quality control procedures were conducted as described previously and detailed in Supplementary information.^{35–37} To implement the extreme-trait design, subjects for initial analysis were selected by evaluating their loss over 2 years in hippocampal volume, measured by magnetic resonance imaging.³⁸ A paired design was employed with all 16 Caucasian, non-Hispanic male subjects having a diagnosis of MCI at the baseline visit and *APOE* $\epsilon 3/\epsilon 3$ genotype. The eight pairs were matched on approximate age, education level, and handedness. One member of each pair had a relatively rapid loss in hippocampal volume over the first 2 years of the study ('rapid rate of atrophy' or *rapid* group) and the other member of each pair had a stable or relatively

slow rate of loss in hippocampal volume over the first 2 years of the study ('slower rate of atrophy' or *slow* group).

WES analysis

WES was performed on blood-derived genomic DNA samples (Supplementary information). Exonic sequences were enriched through hybridization using Agilent's SureSelect Human All Exon 50 Mb kit and sequenced on the Illumina HiSeq2000 using paired-end read chemistry and read lengths of at least 105 bp. Short-read sequences in the target region were mapped to the NCBI reference human genome (build 37.64) using BWA (Burrows-Wheeler Aligner)³⁹ and GATK (Genome Analysis ToolKit) (Supplementary information).⁴⁰ The GATK module, UnifiedGenotyper, was used for multi-sample variant calling. All the variants were annotated with ANNOVAR.⁴¹ PolyPhen-2 and SIFT were used to predict potential impact on protein structure or function of missense variants.^{42,43} Among all exonic variants identified by WES, we specifically focused on identification of variants carried only in the *rapid* group. We analyzed variants in coding regions in which more than four of eight subjects in the *rapid* group had at least one alternative allele, but where all eight subjects in the *slow* group had the same alleles at the locus as the NCBI reference human genome.

Imaging processing

As detailed in previous studies^{38,44,45} and Supplementary information, two widely employed automated magnetic resonance imaging analysis techniques were independently used to process magnetic resonance imaging scans: whole-brain voxel-based morphometry (VBM) using SPM5⁴⁶ and FreeSurfer V4/V5.^{38,44}

Imaging genetics analysis

We investigated further the association discovered from WES using the remaining 315 ADNI-1 *APOE* 3/3 participants, excluding those used for WES, and quantitative imaging phenotypes. We performed imaging genetics analyses using both longitudinal and cross-sectional (baseline) imaging phenotypes. Based on prior studies indicating that atrophy rates for left and right hippocampal volume are different during the progression of AD, we evaluated the associations separately for left and right hippocampal volume.^{47,48} Multivariate analyses of cortical thickness and gray-matter (GM) density were performed to examine genotype effects of candidate single nucleotide variants (SNVs) identified by WES on vertex-by-vertex and voxel-by-voxel bases, respectively. We used age at baseline, gender, years of education, and total intracranial volume as covariates (Supplementary information).

Meta-analysis

We performed a meta-analysis for SNVs identified from WES using the ADNI-1, subsequent extension of ADNI, AddNeuroMed, Indiana Memory and Aging Study, and Multi Institutional Research on Alzheimer Genetic Epidemiology studies to validate the association with hippocampal volume. OpenMeta and METAL were used for the meta-analysis with a fixed-effect inverse variance model.^{49,50}

RESULTS

Sample characteristics are presented in Supplementary Table S1. By design, groups differed in the rate of change in hippocampal volume ($P < 0.001$). However, there was no significant difference in mean values of demographic variables between 16 MCIs used for WES and the remaining ADNI-1 MCI group ($N = 347$) (Supplementary Table S2).

WES and mapping

In Supplementary Table S3, sequencing and mapping statistics are presented for the 16 exomes. On average, we generated 161 million reads for each individual exome, of which 136 million reads (84%) were uniquely mapped to the NCBI human reference sequence (Build 37). The average rate of bases mismatching the reference for all bases aligned to the reference sequence was 0.36%, indicating that the data were of high sequencing quality. The average coverage of each base in the target regions was 40×. Overall, 79.9% of all bases mapped uniquely to target regions were sufficiently deeply covered with a minimum sequencing depth of 30×.

Identification of SNVs and short insertion/deletions (indels)

To identify genetic variants associated with rate of hippocampal volume loss with evidence for an alternative allele present among individuals, we used multi-sample variant calling.⁴⁰ Variants were restricted to bases within the target regions that received a Phred-based quality score of ≥ 30 . After initial variant calling, variant quality score recalibration was performed.⁴⁰ We identified 89 400 SNVs, of which 5941 (6.6%) were not found in the dbSNP database (dbSNP135) and hence were regarded as novel. Before further analysis, the quality of the variant calls was assessed by (1) calculating the transition-to-transversion ratio (ts/tv); and (2) comparing sequencing-derived SNVs with those obtained from the Illumina genotyping array. The ts/tv ratio for all of the SNVs detected in our exomes was 2.72, but the observed ts/tv ratio for SNVs in the coding region was 3.14, within the expected range for coding sequences.⁴⁰ To determine concordance between the sequence-based genotype calls and the 610-Quad array-based chip genotype calls, we analyzed the total number of SNVs called in the target region from the sequencing data that were present in those called by the array. Genotypes determined by sequencing and the chip were 99.4% concordant. Of 89 400 SNVs, there were 50 396 exonic, 945 splicing, and 29 236 intronic SNVs (Supplementary Table S4). In the protein-coding regions, we found 25 144 non-synonymous and 25 234 synonymous SNVs.

Comparison of exomes of rapid and slow groups

Among variants identified from WES, analyses focused on 25 144 exonic non-synonymous SNVs and 613 indels, and 945 SNVs and 82 indels within the regions of the splice site to identify variants associated with rate of hippocampal volume loss in *APOE* 3/3 MCI participants. We determined the frequency of variants in the slow and rapid groups and identified variants carried only by the rapid group. We set our initial threshold for variants of interest as more than four of eight subjects in the rapid group that have at least one alternative allele, but eight subjects in the slow group had the same alleles at the locus as the NCBI human reference sequence. In all, 57 non-synonymous SNVs and one indel in the coding regions were found in at least 4 of 8 subjects in the rapid group but not in any of the 8 subjects in the slow group. Of 57 non-synonymous SNVs identified in this manner, which were all found in the dbSNP database (dbSNP135), those that were present in 6 subjects in the rapid group but not in 8 subjects in the slow group were rs9610775 (*CARD10*), rs1136410 (*PARP1*) and rs6949082 (*HYAL4*) (Supplementary Table S5). rs9610775 and rs1136410 were predicted as ‘probably damaging’ missense variants by PolyPhen-2, and ‘tolerated’ and ‘damaging’ missense variants by SIFT, respectively. rs9610775 and rs1136410 have a minor allele frequency of larger than 10% in the European American population from the National Heart, Lung, and Blood Institute Exome Sequencing Project Database (<https://esp.gs.washington.edu/drupal>). These two SNVs present in 6/8 subjects of the rapid group and absent in 8 subjects of the slow group were selected for further investigation. In the following analyses, we focused on these two SNVs to study further whether they are associated with structural imaging phenotypes of AD-related brain regions in a larger sample, independent from the WES discovery sample.

Quantitative trait analysis (QTL) of hippocampal regions of interest (ROIs)

We investigated further the association discovered with the two SNVs described above by conducting a QTL using the remaining 315 ADNI-1 *APOE* 3/3 participants and quantitative imaging phenotypes. Of newly identified variants, those not genotyped on the Illumina Chip were imputed in the full ADNI-1 sample set using IMPUTE2.⁵¹ Of the two SNVs tested (rs9610775 and rs1136410), rs1136410 showed an association with both the slope and annual percent of change (APC) of right hippocampal volume loss in the 135 ADNI-1 *APOE* 3/3 MCI participants ($P < 0.05$). rs1136410 also showed association with left hippocampal volume only in the 315 ADNI-1 *APOE* 3/3 participants ($P = 0.049$). rs9610775 was found to be associated with hippocampal volume both in the 135 ADNI-1 *APOE* 3/3 MCI participants and in the 315 ADNI-1 *APOE* 3/3 participants ($P < 0.05$) (Table 1).

Surface-based analysis: SurfStat

Figure 1a displays the results of the main adverse effect of rs9610775 (CC>TC>TT; minor allele: T) using baseline magnetic resonance imaging scans. Highly significant clusters associated with rs9610775 were found in bilateral temporal cortical regions, where mean cortical thickness decreased as the dosage of the minor allele (T) of rs9610775 increased. The opposite contrast, the positive effect of rs9610775 (CC<TC<TT), did not show any significant cluster. Figure 2a shows the dominant effect of rs9610775 on rate of cortical thickness loss (slope) over 2 years (CC>TC, TT). A highly significant cluster associated with rs9610775 was found in the left temporal cortical region, as in the WES analysis. Subjects carrying at least one minor allele (T) showed rapid cortical thickness loss over 2 years compared with the participants carrying no minor allele. Figure 3a displays the results of the negative association between rs1136410 and cortical thickness. The most significant cluster associated with rs1136410 was found in right entorhinal cortex with decreased cortical thickness associated with the dosage of the minor allele of rs1136410. No regions were observed at the same statistical threshold in the positive contrast. No significant cortical regions were associated with rate of cortical thickness loss (slope) over 2 years for rs1136410.

Voxel-based analysis: VBM

The VBM results were similar in association direction and regional distribution to those obtained from the cortical thickness analyses. The voxel-wise association between rs9610775 and GM density is shown in Figure 1b. Increased dosage of the minor allele (T) of rs9610775 was associated with reduced GM density. Figure 2b displays the voxel-based analysis results of the dominant association between rs9610775 and rate of GM density loss (slope) over 2 years. An association was observed in the hippocampus. The significant negative association between the genotype of rs1136410 and GM density was also observed in the bilateral inferior temporal lobe (Figure 3b).

Meta-analysis

A meta-analysis result from the five independent cohorts indicated that there is a significant association of rs1136410 with left and right hippocampal volume at baseline ($P = 0.0006$ – 0.0205 ; Table 2 and Supplementary Figures S1–S3).

DISCUSSION

WES was performed in *APOE* 3/3 males with MCI to identify coding variants beyond *APOE* associated with rate of neurodegeneration as defined by rate of change in structural imaging. A subset of variants identified from WES were imputed in non-Hispanic Caucasian

participants from five independent cohorts, and assessed in relation to selected neuroimaging phenotypes from *APOE* 3/3 participants, excluding those used in the WES discovery phase.

We identified 57 non-synonymous SNVs that were found in at least 4 of 8 subjects in the rapid group, but not in any of the 8 subjects in the slow group. Among these SNVs, the variants that accounted for the greatest group difference and were predicted as ‘probably damaging’ missense variants were rs9610775 (*CARD10*) and rs1136410 (*PARP1*). In the ROI-based QTL to investigate the findings further, rs1136410 was significantly associated with the slope and annual percentage change (APC) of hippocampal volume loss in the 135 ADNI-1 *APOE* 3/3 MCI participants. Furthermore, the meta-analysis result from the five independent studies indicated that rs1136410 also showed a significant association with hippocampal volume at baseline in *APOE* 3/3 individuals.

In the whole-brain analysis, the results of both VBM and surface-based analyses for the association of rs9610775 and rs1136410 with brain structure at baseline were consistent. Focal patterns of significant associations with GM density and cortical thickness were observed in the bilateral hippocampus and entorhinal cortex. Regional brain atrophy occurs initially and most severely in the entorhinal cortex and hippocampus before spreading throughout the entire brain.⁵² In the significant clusters, mean cortical thickness and GM density decreased as the dosage of the minor alleles of the two SNVs increased. Thus, the minor allele appears to be a risk factor, as expected. No significant associations were observed between rs1136410 and rates of the cortical thickness and GM density loss in the whole-brain analysis, similar to the QTL. However, highly significant associations of rs9610775 with rate of the cortical thickness and GM density losses over a 2-year period were observed in the left temporal lobe and hippocampus. As in the WES result, subjects carrying at least one minor allele showed rapid cortical thickness and hippocampal volume loss compared with those carrying no minor allele. These findings support rs1136410 and rs9610775 as risk markers for accelerated neurodegeneration. Whole-brain analysis results demonstrated that a voxel-wide and/or surface-based analysis complements a target region of interest method by detecting additional regions of association in an unbiased way.

The missense variant rs9610775 is located in exon 4 of *CARD10* (Caspase recruitment domain family, member 10) on chromosome 22. *CARD10* is expressed in a broad range of tissues, especially at high levels in the brain, liver, kidney and heart.⁵³ In the human brain, this gene is expressed in numerous regions including the hippocampus.⁵⁴ *CARD10* has been shown to be involved in the regulation of caspase activation and apoptosis and assembly of membrane-associated signaling complexes.⁵⁵ *CARD10* is known to activate nuclear factor-kappa B (NF- κ B).^{56–58} NF- κ B, a transcription factor controlling inflammation, is activated in AD brains, predominantly in neurons and glial cells in beta-amyloid plaque surrounding areas.⁵⁹ The NF- κ B signaling pathway has a key role in the development of normal central nervous system, possibly via positive regulation of neuronal survival, and in various neurodegenerative diseases such as AD.^{59,60} However, this gene has not previously been associated with AD or neurodegeneration.

The variant rs1136410 is located at codon 762 in exon 17 of *PARP1* (Poly(ADP-ribose) polymerase-1) on chromosome 1. The gene consists of 23 exons, and spans 47.3 kb. *PARP1* is functionally involved in diverse cellular processes such as DNA damage detection and repair, cell proliferation and death, and maintaining genomic stability.^{61–67} In the human brain, this gene is expressed in numerous regions including the hippocampus.⁵⁴ *PARP1* has been shown to have an important role in long-term memory formation.^{68,69} Love *et al.*⁷⁰ reported enhanced poly(ADP-ribose) polymerase (PARP) activity in the brains of AD patients, particularly in the frontal and temporal lobes. Abeti *et al.*⁷¹ demonstrated that

PARP is activated by oxidative stress and beta-amyloid-induced neuronal death is mediated by PARP in response to oxidative stress. Strosznajder *et al.* suggested that *PARP1* overactivation can be responsible for necrotic cell death, leading to cognitive impairment, and the *PARP1* activation by oxidative stress seems to be an early and important event in the pathogenesis of AD.^{61,72,73} Nevertheless, genetic analysis of association of rs1136410 with the risk of AD produced negative results.^{67,74} Interestingly, *CARD10* activates NF- κ B and *PARP1* is involved in beta-amyloid-induced microglia activation through the regulation of NF- κ B,⁷⁵ implicating a possible common pathway for these variants.

There are a number of strengths of the present study. This is the first study to use WES to identify AD or MCI risk genes and to employ longitudinal change in hippocampal volume as a quantitative trait for WES in an extreme-trait design. We focused on baseline MCI subjects with *APOE* ϵ 3/ ϵ 3 to study an early part of the disease spectrum and identify candidate genes beyond *APOE*, the most significant known genetic risk factor for AD. In addition, multiple refined whole-brain imaging analyses were performed to further characterize the neuroanatomical structures associated with candidate variants in a larger sample. Finally, we performed a meta-analysis using five independent cohorts. Although mitigated somewhat by the extreme-trait design, a limitation of the present report is that available resources only permitted us to sequence 16 exomes, a modest sample size for genetic analysis. In the 16 WES data set, as it is not possible to reach significance after Bonferroni correction for any variant, we could not perform a statistical test using 16 WES data. In addition, WES does not cover all exons, promoters or regulatory regions and this approach may have missed other variants. Future WGS will address these genomic regions with greater coverage.

In summary, we conducted a WES analysis in a small, highly selected number of samples from ADNI-1 with MCI and *APOE* ϵ 3/ ϵ 3, and then carried out cross-sectional and longitudinal quantitative trait and whole-brain analyses to investigate candidate variants further in five independent cohorts. Our findings offer further evidence from a novel approach that *PARP1* and *CARD10* may be associated with neurodegeneration in those at high risk for AD. Importantly, our results implicated these genes independent of any role of *APOE* ϵ 4, since we restricted our search to ϵ 3 homozygotes. Furthermore, rs1136410 (*PARP1*) is also significantly associated with hippocampal volume at baseline in *APOE* ϵ 3/ ϵ 3 individuals. Confirmation of our longitudinal results in independent and larger cohorts remains of critical importance. Overall, combining next-generation sequencing and quantitative imaging phenotypes holds promise for discovery of variants involved in neurodegeneration and other brain disorders.

Supplementary Material

Refer to Web version on PubMed Central for supplementary material.

Acknowledgments

Data collection and sharing for this project was funded by the Alzheimer's Disease Neuroimaging Initiative (ADNI) (National Institutes of Health Grant U01 AG024904) (Supplementary information).

References

1. Thies W, Bleiler L. Alzheimer's disease facts and figures. *Alzheimers Dement* 2011. 2011; 7:208–244.
2. Blennow K, de Leon MJ, Zetterberg H. Alzheimer's disease. *Lancet*. 2006; 368:387–403. [PubMed: 16876668]

3. Hardy J, Selkoe DJ. The amyloid hypothesis of Alzheimer's disease: progress and problems on the road to therapeutics. *Science*. 2002; 297:353–356. [PubMed: 12130773]
4. Bergem AL. Heredity in dementia of the Alzheimer type. *Clin Genet*. 1994; 46(1 Spec):144–149. [PubMed: 7988071]
5. Bergem AL, Engedal K, Kringlen E. The role of heredity in late-onset Alzheimer disease and vascular dementia. A twin study. *Arch Gen Psychiatry*. 1997; 54:264–270. [PubMed: 9075467]
6. Gatz M, Pedersen NL, Berg S, Johansson B, Johansson K, Mortimer JA, et al. Heritability for Alzheimer's disease: the study of dementia in Swedish twins. *J Gerontol A Biol Sci Med Sci*. 1997; 52:M117–M125. [PubMed: 9060980]
7. Bertram L, Tanzi RE. Thirty years of Alzheimer's disease genetics: the implications of systematic meta-analyses. *Nat Rev Neurosci*. 2008; 9:768–778. [PubMed: 18802446]
8. Abraham R, Moskvina V, Sims R, Hollingworth P, Morgan A, Georgieva L, et al. A genome-wide association study for late-onset Alzheimer's disease using DNA pooling. *BMC Med Genomics*. 2008; 1:44. [PubMed: 18823527]
9. Beecham GW, Martin ER, Li YJ, Slifer MA, Gilbert JR, Haines JL, et al. Genome-wide association study implicates a chromosome 12 risk locus for late-onset Alzheimer disease. *Am J Hum Genet*. 2009; 84:35–43. [PubMed: 19118814]
10. Bertram L, Lange C, Mullin K, Parkinson M, Hsiao M, Hogan MF, et al. Genome-wide association analysis reveals putative Alzheimer's disease susceptibility loci in addition to APOE. *Am J Hum Genet*. 2008; 83:623–632. [PubMed: 18976728]
11. Harold D, Abraham R, Hollingworth P, Sims R, Gerrish A, Hamshere ML, et al. Genome-wide association study identifies variants at CLU and PICALM associated with Alzheimer's disease. *Nat Genet*. 2009; 41:1088–1093. [PubMed: 19734902]
12. Lambert JC, Heath S, Even G, Campion D, Sleegers K, Hiltunen M, et al. Genome-wide association study identifies variants at CLU and CR1 associated with Alzheimer's disease. *Nat Genet*. 2009; 41:1094–1099. [PubMed: 19734903]
13. Jun G, Naj AC, Beecham GW, Wang LS, Buross J, Gallins PJ, et al. Meta-analysis confirms CR1, CLU, and PICALM as Alzheimer disease risk loci and reveals interactions with APOE genotypes. *Arch Neurol*. 2010; 67:1473–1484. [PubMed: 20697030]
14. Seshadri S, Fitzpatrick AL, Ikram MA, DeStefano AL, Gudnason V, Boada M, et al. Genome-wide analysis of genetic loci associated with Alzheimer disease. *JAMA*. 2010; 303:1832–1840. [PubMed: 20460622]
15. Naj AC, Jun G, Beecham GW, Wang LS, Vardarajan BN, Buross J, et al. Common variants at MS4A4/MS4A6E, CD2AP, CD33 and EPHA1 are associated with late-onset Alzheimer's disease. *Nat Genet*. 2011; 43:436–441. [PubMed: 21460841]
16. Hollingworth P, Harold D, Sims R, Gerrish A, Lambert JC, Carrasquillo MM, et al. Common variants at ABCA7, MS4A6A/MS4A4E, EPHA1, CD33 and CD2AP are associated with Alzheimer's disease. *Nat Genet*. 2011; 43:429–435. [PubMed: 21460840]
17. Corder EH, Saunders AM, Strittmatter WJ, Schmechel DE, Gaskell PC, Small GW, et al. Gene dose of apolipoprotein E type 4 allele and the risk of Alzheimer's disease in late onset families. *Science*. 1993; 261:921–923. [PubMed: 8346443]
18. Farrer LA, Cupples LA, Haines JL, Hyman B, Kukull WA, Mayeux R, et al. Effects of age, sex, and ethnicity on the association between apolipoprotein E genotype and Alzheimer disease. A meta-analysis. APOE and Alzheimer Disease Meta Analysis Consortium. *JAMA*. 1997; 278:1349–1356. [PubMed: 9343467]
19. Bu G, Apolipoprotein E. and its receptors in Alzheimer's disease: pathways, pathogenesis and therapy. *Nat Rev Neurosci*. 2009; 10:333–344. [PubMed: 19339974]
20. So HC, Gui AH, Cherny SS, Sham PC. Evaluating the heritability explained by known susceptibility variants: a survey of ten complex diseases. *Genet Epidemiol*. 2011; 35:310–317. [PubMed: 21374718]
21. Manolio TA, Collins FS, Cox NJ, Goldstein DB, Hindorf LA, Hunter DJ, et al. Finding the missing heritability of complex diseases. *Nature*. 2009; 461:747–753. [PubMed: 19812666]
22. Cirulli ET, Goldstein DB. Uncovering the roles of rare variants in common disease through whole-genome sequencing. *Nat Rev Genet*. 2010; 11:415–425. [PubMed: 20479773]

23. Cooper GM, Shendure J. Needles in stacks of needles: finding disease-causal variants in a wealth of genomic data. *Nat Rev Genet.* 2011; 12:628–640. [PubMed: 21850043]
24. Ng SB, Buckingham KJ, Lee C, Bigham AW, Tabor HK, Dent KM, et al. Exome sequencing identifies the cause of a mendelian disorder. *Nat Genet.* 2010; 42:30–35. [PubMed: 19915526]
25. Holm H, Gudbjartsson DF, Sulem P, Masson G, Helgadóttir HT, Zanon C, et al. A rare variant in MYH6 is associated with high risk of sick sinus syndrome. *Nat Genet.* 2011; 43:316–320. [PubMed: 21378987]
26. Choi M, Scholl UI, Ji W, Liu T, Tikhonova IR, Zumbo P, et al. Genetic diagnosis by whole exome capture and massively parallel DNA sequencing. *Proc Natl Acad Sci USA.* 2009; 106:19096–19101. [PubMed: 19861545]
27. Klein CJ, Botuyan MV, Wu Y, Ward CJ, Nicholson GA, Hammans S, et al. Mutations in DNMT1 cause hereditary sensory neuropathy with dementia and hearing loss. *Nat Genet.* 2011; 43:595–600. [PubMed: 21532572]
28. Kim JJ, Park YM, Baik KH, Choi HY, Yang GS, Koh I, et al. Exome sequencing and subsequent association studies identify five amino acid-altering variants influencing human height. *Human Genet.* 2012; 131:471–478. [PubMed: 21959382]
29. Pottier C, Hannequin D, Coutant S, Rovelet-Lecrux A, Wallon D, Rousseau S, et al. High frequency of potentially pathogenic SORL1 mutations in autosomal dominant early-onset Alzheimer disease. *Mol Psychiatry.* 2012; 17:875–879. [PubMed: 22472873]
30. Guerreiro RJ, Lohmann E, Kinsella E, Bras JM, Luu N, Gurlunlian N, et al. Exome sequencing reveals an unexpected genetic cause of disease: NOTCH3 mutation in a Turkish family with Alzheimer’s disease. *Neurobiol Aging.* 2012; 33:1008 e1017–1008 e1023. [PubMed: 22153900]
31. Bettens K, Brouwers N, Engelborghs S, Lambert JC, Rogaeva E, Vandenberghe R, et al. Both common variations and rare non-synonymous substitutions and small insertion/deletions in CLU are associated with increased Alzheimer risk. *Mol Neurodegener.* 2012; 7:3. [PubMed: 22248099]
32. Ferrari R, Moreno JH, Minhajuddin AT, O’Bryant SE, Reisch JS, Barber RC, et al. Implication of common and disease specific variants in CLU, CR1, and PICALM. *Neurobiol Aging.* 2012; 33:1846. [PubMed: 22402018]
33. Petersen RC, Smith GE, Waring SC, Ivnik RJ, Tangalos EG, Kokmen E. Mild cognitive impairment: clinical characterization and outcome. *Arch Neurol.* 1999; 56:303–308. [PubMed: 10190820]
34. Petersen RC, Roberts RO, Knopman DS, Boeve BF, Geda YE, Ivnik RJ, et al. Mild cognitive impairment: ten years later. *Arch Neurol.* 2009; 66:1447–1455. [PubMed: 20008648]
35. Saykin AJ, Shen L, Foroud TM, Potkin SG, Swaminathan S, Kim S, et al. Alzheimer’s Disease Neuroimaging Initiative biomarkers as quantitative phenotypes: genetics core aims, progress, and plans. *Alzheimer’s Dement.* 2010; 6:265–273. [PubMed: 20451875]
36. Kim S, Swaminathan S, Shen L, Risacher SL, Nho K, Foroud T, et al. Genome-wide association study of CSF biomarkers Aβ₁₋₄₂, t-tau, and p-tau_{181p} in the ADNI cohort. *Neurology.* 2011; 76:69–79. [PubMed: 21123754]
37. Weiner MW, Veitch DP, Aisen PS, Beckett LA, Cairns NJ, Green RC, et al. The Alzheimer’s Disease Neuroimaging Initiative: a review of papers published since its inception. *Alzheimers Dement.* 2012; 8(1 Suppl):S1–68. [PubMed: 22047634]
38. Risacher SL, Shen L, West JD, Kim S, McDonald BC, Beckett LA, et al. Longitudinal MRI atrophy biomarkers: relationship to conversion in the ADNI cohort. *Neurobiol Aging.* 2010; 31:1401–1418. [PubMed: 20620664]
39. Li H, Durbin R. Fast and accurate short read alignment with Burrows-Wheeler transform. *Bioinformatics.* 2009; 25:1754–1760. [PubMed: 19451168]
40. DePristo MA, Banks E, Poplin R, Garimella KV, Maguire JR, Hartl C, et al. A framework for variation discovery and genotyping using next-generation DNA sequencing data. *Nat Genet.* 2011; 43:491–498. [PubMed: 21478889]
41. Wang K, Li M, Hakonarson H. ANNOVAR: functional annotation of genetic variants from high-throughput sequencing data. *Nucleic Acids Res.* 2010; 38:e164. [PubMed: 20601685]
42. Adzhubei IA, Schmidt S, Peshkin L, Ramensky VE, Gerasimova A, Bork P, et al. A method and server for predicting damaging missense mutations. *Nat Meth.* 2010; 7:248–249.

43. Kumar P, Henikoff S, Ng PC. Predicting the effects of coding non-synonymous variants on protein function using the SIFT algorithm. *Nat Protoc.* 2009; 4:1073–1081. [PubMed: 19561590]
44. Risacher SL, Saykin AJ, West JD, Shen L, Firpi HA, McDonald BC. Baseline MRI predictors of conversion from MCI to probable AD in the ADNI cohort. *Curr Alzheimer Res.* 2009; 6:347–361. [PubMed: 19689234]
45. Jack CR Jr, Bernstein MA, Fox NC, Thompson P, Alexander G, Harvey D, et al. The Alzheimer's Disease Neuroimaging Initiative (ADNI): MRI methods. *J Magn Reson Imaging.* 2008; 27:685–691. [PubMed: 18302232]
46. Ashburner J, Friston KJ. Voxel-based morphometry--the methods. *NeuroImage.* 2000; 11(6 Pt 1): 805–821. [PubMed: 10860804]
47. Brand K, Eisele T, Kreusel U, Page M, Page S, Haas M, et al. Dysregulation of monocytic nuclear factor-kappa B by oxidized low-density lipoprotein. *Arterioscler Thromb Vasc Biol.* 1997; 17:1901–1909. [PubMed: 9351352]
48. Muller JM, Krauss B, Kaltschmidt C, Baeuerle PA, Rupec RA. Hypoxia induces c-fos transcription via a mitogen-activated protein kinase-dependent pathway. *J Biol Chem.* 1997; 272:23435–23439. [PubMed: 9287359]
49. Barnes LL, Wilson RS, Li Y, Gilley DW, Bennett DA, Evans DA. Change in cognitive function in Alzheimer's disease in African-American and white persons. *Neuro-epidemiology.* 2006; 26:16–22.
50. Barnes J, Scahill RI, Schott JM, Frost C, Rossor MN, Fox NC. Does Alzheimer's disease affect hippocampal asymmetry? Evidence from a cross-sectional and longitudinal volumetric MRI study. *Dement Geriatr Cogn Disord.* 2005; 19:338–344. [PubMed: 15785035]
51. Howie BN, Donnelly P, Marchini J. A flexible and accurate genotype imputation method for the next generation of genome-wide association studies. *PLoS Genet.* 2009; 5:e1000529. [PubMed: 19543373]
52. Scahill RI, Schott JM, Stevens JM, Rossor MN, Fox NC. Mapping the evolution of regional atrophy in Alzheimer's disease: unbiased analysis of fluid-registered serial MRI. *Proc Natl Acad Sci USA.* 2002; 99:4703–4707. [PubMed: 11930016]
53. McAllister-Lucas LM, Inohara N, Lucas PC, Ruland J, Benito A, Li Q, et al. Bim1, a MAGUK family member linking protein kinase C activation to Bcl10-mediated NF-kappaB induction. *J Biol Chem.* 2001; 276:30589–30597. [PubMed: 11387339]
54. Jones AR, Overly CC, Sunkin SM. The Allen Brain Atlas: 5 years and beyond. *Nat Rev Neurosci.* 2009; 10:821–828. [PubMed: 19826436]
55. Wang L, Guo Y, Huang WJ, Ke X, Poyet JL, Manji GA, et al. Card10 is a novel caspase recruitment domain/membrane-associated guanylate kinase family member that interacts with BCL10 and activates NF-kappa B. *J Biol Chem.* 2001; 276:21405–21409. [PubMed: 11259443]
56. Wegener E, Krappmann D. CARD-Bcl10-Malt1 signalosomes: missing link to NF-kappaB. *Science's STKE.* 2007; 2007:pe21.
57. McAllister-Lucas LM, Jin X, Gu S, Siu K, McDonnell S, Ruland J, et al. The CARMA3-Bcl10-MALT1 signalosome promotes angiotensin II-dependent vascular inflammation and atherogenesis. *J Biol Chem.* 2010; 285:25880–25884. [PubMed: 20605784]
58. Sun J. CARMA3: A novel scaffold protein in regulation of NF-kappaB activation and diseases. *World J Biol Chemistry.* 2010; 1:353–361.
59. Kaltschmidt B, Uherek M, Volk B, Baeuerle PA, Kaltschmidt C. Transcription factor NF-kappaB is activated in primary neurons by amyloid beta peptides and in neurons surrounding early plaques from patients with Alzheimer disease. *Proc Natl Acad Sci USA.* 1997; 94:2642–2647. [PubMed: 9122249]
60. Ruland J, Duncan GS, Elia A, del Barco Barrantes I, Nguyen L, Plyte S, et al. Bcl10 is a positive regulator of antigen receptor-induced activation of NF-kappaB and neural tube closure. *Cell.* 2001; 104:33–42. [PubMed: 11163238]
61. Strosznajder JB, Czapski GA, Adamczyk A, Strosznajder RP. Poly(ADP-ribose) polymerase-1 in amyloid beta toxicity and Alzheimer's disease. *Mol Neurobiol.* 2012; 46:78–84. [PubMed: 22430645]

62. Moncada S, Bolanos JP. Nitric oxide, cell bioenergetics and neurodegeneration. *J Neurochem.* 2006; 97:1676–1689. [PubMed: 16805776]
63. Strosznajder RP, Jesko H, Zambrzycka A. Poly(ADP-ribose) polymerase: the nuclear target in signal transduction and its role in brain ischemia-reperfusion injury. *Mol Neurobiol.* 2005; 31:149–167. [PubMed: 15953818]
64. Menissier de Murcia J, Ricoul M, Tartier L, Niedergang C, Huber A, Dantzer F, et al. Functional interaction between PARP-1 and PARP-2 in chromosome stability and embryonic development in mouse. *EMBO J.* 2003; 22:2255–2263. [PubMed: 12727891]
65. Yu SW, Andrabi SA, Wang H, Kim NS, Poirier GG, Dawson TM, et al. Apoptosis-inducing factor mediates poly(ADP-ribose) (PAR) polymer-induced cell death. *Proc Natl Acad Sci USA.* 2006; 103:18314–18319. [PubMed: 17116881]
66. Ba X, Garg NJ. Signaling mechanism of poly(ADP-ribose) polymerase-1 (PARP-1) in inflammatory diseases. *Am J Pathol.* 2011; 178:946–955. [PubMed: 21356345]
67. Liu HP, Lin WY, Wu BT, Liu SH, Wang WF, Tsai CH, et al. Evaluation of the poly(ADP-ribose) polymerase-1 gene variants in Alzheimer's disease. *J Clin Lab Anal.* 2010; 24:182–186. [PubMed: 20486200]
68. Goldberg S, Visochek L, Giladi E, Gozes I, Cohen-Armon M. PolyADP-ribosylation is required for long-term memory formation in mammals. *J Neurochem.* 2009; 111:72–79. [PubMed: 19645746]
69. Cohen-Armon M, Visochek L, Katzoff A, Levitan D, Susswein AJ, Klein R, et al. Long-term memory requires polyADP-ribosylation. *Science.* 2004; 304:1820–1822. [PubMed: 15205535]
70. Love S, Barber R, Wilcock GK. Increased poly(ADP-ribosyl)ation of nuclear proteins in Alzheimer's disease. *Brain.* 1999; 122(Pt 2):247–253. [PubMed: 10071053]
71. Abeti R, Abramov AY, Duchon MR. Beta-amyloid activates PARP causing astrocytic metabolic failure and neuronal death. *Brain.* 2011; 134(Pt 6):1658–1672. [PubMed: 21616968]
72. Kauppinen TM. Multiple roles for poly(ADP-ribose)polymerase-1 in neurological disease. *Neurochem Int.* 2007; 50:954–958. [PubMed: 17222947]
73. Kauppinen TM, Swanson RA. The role of poly(ADP-ribose) polymerase-1 in CNS disease. *Neuroscience.* 2007; 145:1267–1272. [PubMed: 17084037]
74. Infante J, Llorca J, Mateo I, Rodriguez-Rodriguez E, Sanchez-Quintana C, Sanchez-Juan P, et al. Interaction between poly(ADP-ribose) polymerase 1 and interleukin 1A genes is associated with Alzheimer's disease risk. *Dement Geriatr Cogn Disord.* 2007; 23:215–218. [PubMed: 17290104]
75. Kauppinen TM, Suh SW, Higashi Y, Berman AE, Escartin C, Won SJ, et al. Poly(ADP-ribose)polymerase-1 modulates microglial responses to amyloid beta. *J Neuroinfl.* 2011; 8:152.

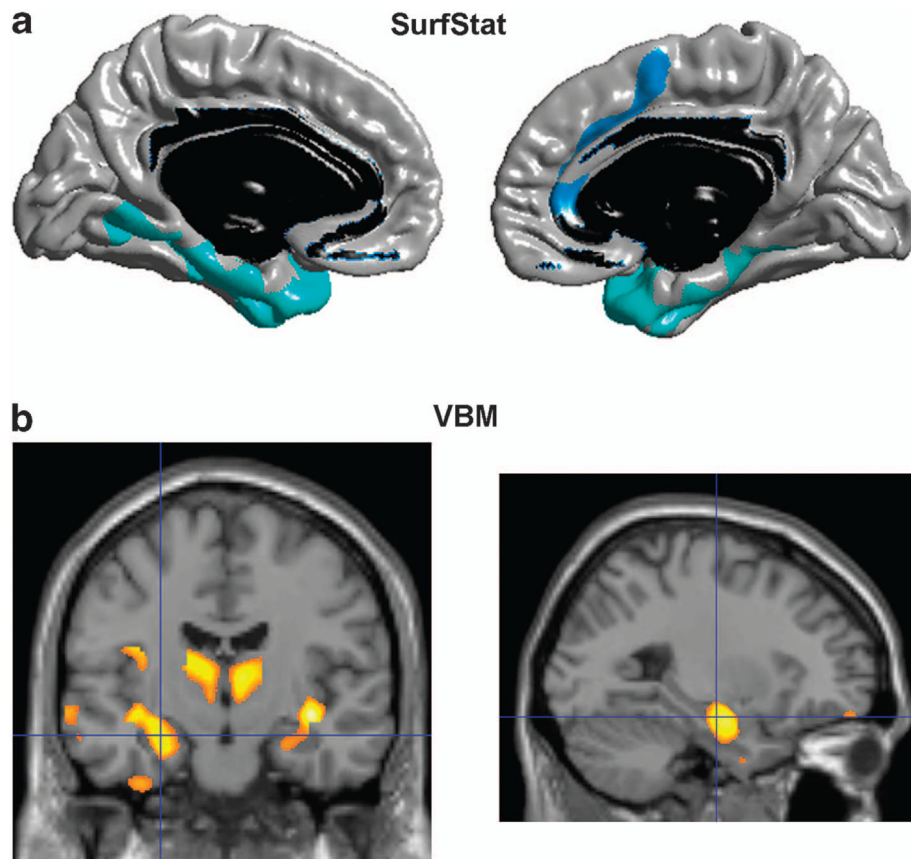


Figure 1. Validation of whole-exome sequencing (WES)-identified variant (rs9610775) in larger sample of 315 Alzheimer's Disease Neuroimaging Initiative Phase 1 (ADNI-1) subjects by surface-based analysis of cortical thickness (a) and voxel-based morphometry (VBM) analysis (b) of gray-matter density at baseline. Statistical maps of SurfStat were thresholded using random field theory (RFT) correction with a corrected significance level of 0.05. The VBM results were presented at $P < 0.05$ (uncorrected). Left hemisphere is shown on the left.

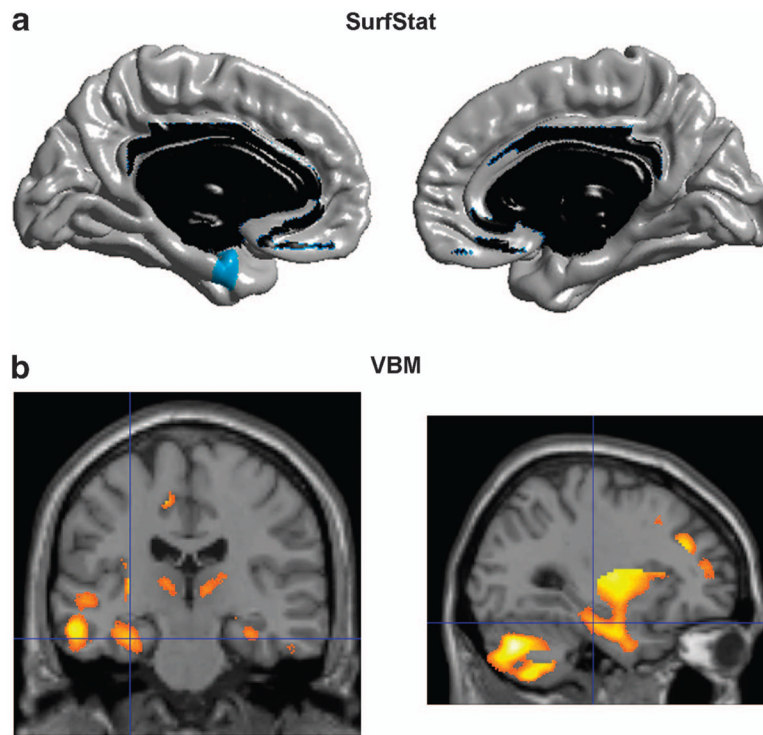


Figure 2. Validation of whole-exome sequencing (WES)-identified variant (rs9610775) using surface-based analysis (a) and voxel-based morphometry (VBM) analysis (b). We showed the dominant effect of rs9610775 on rate of cortical thickness loss (a) and gray-matter density loss (b) over 2 years. Statistical maps of SurfStat were thresholded using random field theory (RFT) correction with a corrected significance level of 0.05. The VBM results are presented at $P < 0.05$ (uncorrected). Left hemisphere is shown on the left.

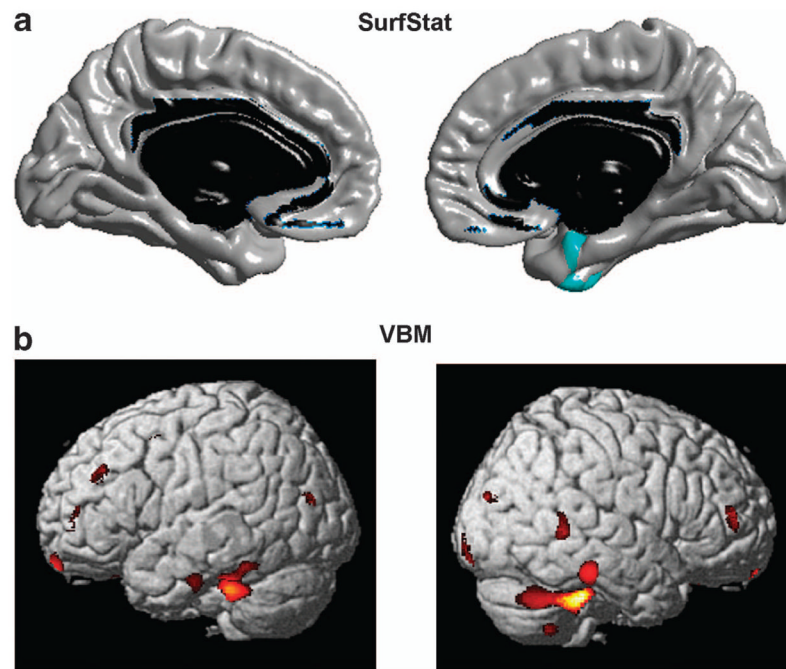


Figure 3. Validation of whole-exome sequencing (WES)-identified variant (rs1136410) using surface-based analysis (a) of cortical thickness and voxel-based morphometry (VBM) analysis (b) of gray-matter density at baseline. Statistical maps of SurfStat were thresholded using random field theory (RFT) correction with a corrected significance level of 0.05. The VBM results are presented at $P < 0.05$ (uncorrected). Left hemisphere is shown on the left.

Table 1Association results (*P*-values) of quantitative trait analysis using a dominant model in ADNI-1

	All APOE 3/3 participants (N =315)		APOE 3/3 MCI (N = 135)	
	rs9610775 (<i>CARD10</i>)	rs1136410 (<i>PARP1</i>)	rs9610775 (<i>CARD10</i>)	rs1136410 (<i>PARP1</i>)
<i>Left hippocampus</i>				
Volume	0.178	0.049	0.023	0.066
APC	0.306	0.529	0.346	0.652
Slope	0.371	0.558	0.811	0.510
<i>Right hippocampus</i>				
Volume	0.020	0.279	0.010	0.164
APC	0.900	0.324	0.998	0.044
Slope	0.790	0.268	0.954	0.034
<i>Mean bilateral hippocampus</i>				
Volume	0.051	0.113	0.011	0.094
APC	0.541	0.836	0.558	0.162
Slope	0.459	0.738	0.808	0.094

Abbreviations: ADNI-1, Alzheimer's Disease Neuroimaging Initiative Phase 1; APC, Annual percentage of change; APOE, apolipoprotein E.

Table 2Association results (*P*-values) of five independent cohorts

Study	rs9610775					rs1136410				
	Left HippoVol	Right HippoVol	Mean HippoVol	Left HippoVol	Right HippoVol	Mean HippoVol	Left HippoVol	Right HippoVol	Mean HippoVol	
ADNI-1 (N=315)	0.178	0.020	0.051	0.049	0.279	0.113				
ADNI-GO-2 (N=205)	0.333	0.039	0.348	0.403	0.058	0.038				
IMAS (N=40)	0.479	0.416	0.588	0.737	0.897	0.744				
AddNeuroMed (N=123)	0.736	0.049	0.784	0.850	0.160	0.078				
MIRAGE (N=240)	0.099	0.127	0.085	0.124	0.624	0.283				
Meta-analysis (N=923)	0.252	0.084	0.122	0.0006	0.0205	0.0026				

Abbreviations: ADNI-1, Alzheimer's Disease Neuroimaging Initiative Phase 1; ADNI-GO-2, Subsequent Extension of Alzheimer's Disease Neuroimaging Initiative; HippoVol, Hippocampal volume; IMAS, Indiana Memory and Aging Study; MIRAGE, Multi Institutional Research on Alzheimer Genetic Epidemiology.